THE NATURE OF SOFT X-RAY EMISSION IN OBSCURED AGN

Matteo Guainazzi, Stefano Bianchi [a]

[a]European Space Astronomy Center of ESA, Apartado 50727, E-28080 Madrid, Spain

We present results of a high-resolution soft X-ray (0.2–2 keV) spectroscopic study on a sample of 66 nearby obscured AGN observed by the Reflection Transmission Grating (RGS) on board XMM-Newton. This is the largest sample ever studied with this technique so far. The main conclusions of our study can be summarized as follows: a) narrow Radiative Recombination Continua are detected in 40% of the objects in our sample; in 27% their width is $\leq$ 10 eV; b) higher order transitions are generally enhanced with respect to pure photoionization, indicating that resonant scattering plays an important role in the ionization/excitation balance. These results support the scenario, whereby the active nucleus is responsible for the X-ray "soft excess" almost ubiquitously observed in nearby obscured AGN via photoionization of circumnuclear gas. They confirm on a statistical basis the conclusions drawn from the detailed study of the brightest spectra in the sample. Furthermore, we propose a criterion to statistically discriminate between AGN-photoionized sources and starbursts galaxies, based on intensity of the forbidden component of the OVII He-α triplet (once normalized to the OVIII Ly-α) coupled with the integrated luminosity in He-like and H-like oxygen lines.

1. Introduction

Nearby X-ray obscured AGN invariably exhibit excess emission above the extrapolation of the absorbed nuclear emission [27,13]. The origin of this component - which can represent a significant fraction of the active nucleus bolometric energy budget [18] - is still largely unknown. Gas in the nuclear environment could be heated to million degrees by shocks induced by AGN outflows [15] or episodes of intense star formation [6,12]. Alternatively, the Active Galactic Nucleus (AGN) primary emission could photoionize and photoexcite circumnuclear gas.

The latter scenario has recently received direct observation support, thanks to high-resolution capabilities in the spatial and frequency domains that large X-ray observatories such as *Chandra* and XMM-Newton nowadays offer. High-resolution spectra unveil signatures of photoionized plasma in a few bright objects: NGC 1068 [16,28], the Circinus Galaxy [23], Mkn 3 [24,3,22]; NGC 4151 [26]. In NGC 1068 the contribution of any collisionally ionized plasma to the observed soft X-ray emission is constrained to be lower then 10% [5]. These conclusions are based on three experimental pieces of evidence:

1. the spectra are dominated by strong emission lines of highly-ionized species from Carbon to Silicon, as well as by L-shell transitions from FeXVII to FeXXI
2. narrow Radiative Recombination Continua (RRC) features from Carbon and Oxygen were detected. The width of these features indicates typical plasma temperatures of the order of a few eV [16]. These features are unequivocal signatures of photoionized spectra [19].
3. the intensity of higher-order series emission lines, once normalized to the K_α, are larger than predicted by pure photoionization, and are consistent with an important contribution by photoexcitation (resonant scattering) [1,20,17]. This explains why standard plasma diagnostics [21] fail to properly interpret the physical nature of the spectra.

A solution in terms of AGN-photoionized gas can as well explain the coincidence in extension and overall morphology between soft X-ray emission and the Narrow Line Regions (NLRs), the latter traced by O[III] HST maps, on scales as large as a few hundreds parsecs [2]. Solutions satisfying the observed X-ray to optical flux ratio require an approximately constant ionization parameter (*i.e.*, a density scaling as the inverse square of the distance from the ionizing source), similarly to what often found by photoionization models of the NLRs.

So far, high-resolution X-ray spectra have been published for a few X-ray bright obscured AGN only. However, diagnostically important emission

lines in these objects exhibit very large Equivalent Widths, *EW*s, as the continuum is often totally suppressed in this energy band. In this *paper* we present the first systematic high-resolution X-ray spectroscopic study on a sizable sample of obscured AGN. The Reflection Grating Spectrometer (RGS) on board XMM-Newton [8] is the most suitable instrument currently flying for this purpose, due to its unprecedented effective area in the 0.2-2 keV keV, as well as to its good absolute aspect solution accuracy ($\simeq$8 mÅ).

2. *CIELO*

Our sample comprises all the type $\geq$1.5 AGN (according to the NED classification) observed by XMM-Newton, and whose data are public as of December 2005. The sample comprises 66 sources. For each observation, we have reprocessed RGS data with SASv6.5 [11] using the most advanced calibration files available as of May 2006. Background spectra were generated using blank fields event list, accumulated from different positions on the sky vault along the mission. Spectra of the same source from different observations have been merged, alongside their response matrices, after checking that no significant spectral variability occurred. Each spectrum has been searched for the presence of emission lines. "Local" fits to the data have been performed on the unbinned spectra on $\simeq$100 channels wide intervals, using unresolved Gaussian profiles to account for any emission line features. No assumption has been made *a priori* on the line centroid energies.[1] The local continua have been modeled with power-laws. Line luminosities have been corrected for Galactic photoelectric absorption using column densities after Dickey & Lockman (1990). In Fig. 1 we show the RGS spectra of the three still unpublished Seyfert 2 galaxies in our sample, which exhibit the largest number of line detections. All spectra exhibits a prominent OVII K_α triplet, largely dominated by the forbidden (f) transition, with a weak resonance (r) and a negligible intercombination (i) transition.

The results of the procedure outlined above have been compiled into **CIELO-AGN** (*Catalog of Ionized Emission Lines in Obscured AGN*). Despite the overall low soft X-ray flux (sample median $\sim 10^{-13}$ erg cm^{-2} s^{-1}), the OVIII Ly-α

[1] On the other hand, upper limits on the line intensities have been calculated assuming the laboratory energies.

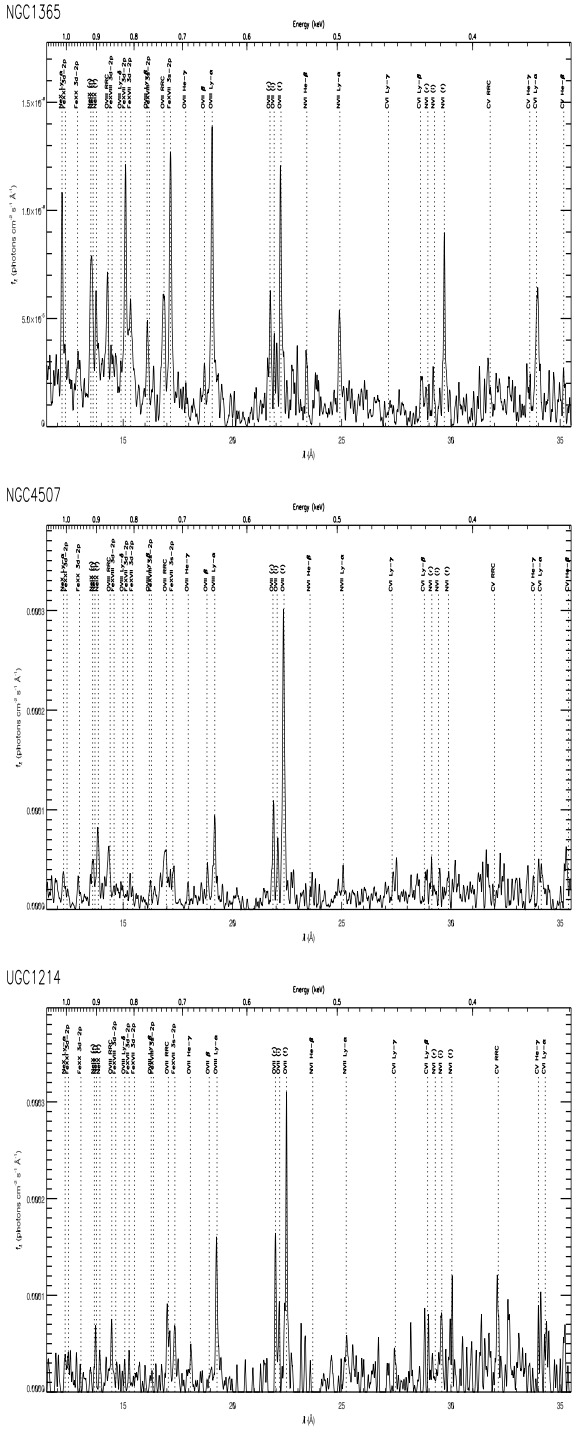

Figure 1. RGS spectra for the three galaxies of our sample, which exhibit the largest number of detected emission lines (in brackets below) and whose RGS spectra have not been published yet: NGC 1365 (19), NGC 4507 (17), UGC 1214 (14) [for comparison the number of detected lines in the brightest Seyfert 2 of our samples are: 25 (NGC 1068), 19 (the Circinus Galaxy), 18 (NGC 4151), 17 (Mrk 3)]. Spectra have been smoothed with a 5-channels wide triangular kernel for illustration purposes only. The position of the line transitions measured in *CIELO* is labeled.

is detected in 44% (29/66) objects of the sample, whereas at least one component of the OVII He-α triplet in 36%. In 25-35% of the sample objects He- and H-like Neon transitions are detected, as well as L-shell transitions from FeXVIII to FeXXI. Several other Carbon and Silicon lines are detected in $\leq$ 15% of the sample objects. In no case a significant difference between the rest frame line centroid and the laboratory energy has been found.

Hereafter, uncertainties are quoted at the 1σ level; energies are quoted in the source rest frame, unless otherwise specified.

3. Results

In this Section we will use some results of our study to try and answer the following questions on the nature of soft X-ray emission in obscured AGN:

- is AGN photoionization the dominant physical process?
- does resonant scattering play an important role?
- do efficient X-ray line diagnostics exist, which could allow us to discriminate on a statistical basis between AGN- and starburst-powered spectra?

3.1. RRC

The three most intense RRCs transitions in the RGS energy bandpass are: OVIII at 14.235Å, OVII at 16.777Å and CV at 31.622Å. At least one of these features is detected in 40% (24/66) of the objects of our sample. The few measurements of the RRC width, which represents a direct estimate of the temperature of the plasma [19], cluster in the range 1–10 eV. There is an obvious selection effect, favouring the detection of narrow features. Nonetheless, still in 33% (27%) of the objects in our sample the RRC width is constrained to be lower than 50 (10) eV (see Fig. 2). In 10 further objects we detect upper limits on the RRC luminosity in the range where measurements are found: in 7 (10) of them the luminosity is constrained to be $\leq 10^{41.1}$ erg s^{-1} ($\leq 10^{44.2}$ erg s^{-1}). Finally, in 32/66 (48%) of the objects the quality of the data is too poor to allow a significant detection of any of the RRC features, and the upper limits on their luminosities are inconclusive.

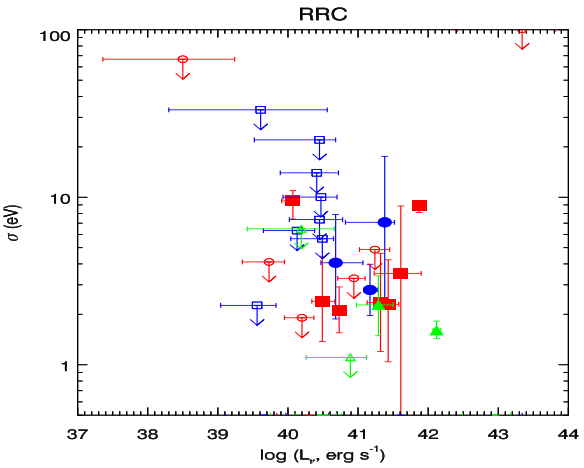

Figure 2. Luminosity versus width for the RRC features detected in our sample. *Filled* data points correspond to a measurement of the RRC width; *empty* data points correspond to RRC width upper limits. *Circles*: OVIII; *squares*: OVII; *triangles*: CV. Data points corresponding to upper limits on both quantities are not shown for clarity.

3.2. Higher order series

In addition to $n = 2p \rightarrow 1s$ transitions for H- and He-like atoms, *CIELO* contains a fair amount of detection of discrete higher order resonance transitions ($np \rightarrow 1s, n > 2$). These transitions are selectively enhanced by photoexcitation. Since the forbidden f transition in He-like triplets is unaffected by photoexcitation, the intensity ratio between higher order series and f transition intensities provides a potentially powerful diagnostic of the importance of resonant scattering in radiation ionized spectra [16]. An example of the application of this diagnostic to *CIELO* is shown in Fig. 3, where we display the intensity of the OVII He-β against the f component of the OVII He-α triplet. We compare the experimental results with the predictions of pure photoionization, and with models where radiative decay from photoexcitation and recombination from photoionization are self-consistently calculated (model `photoion`; Kinkhabwala et al. 2002). We have produced a grid of models for different values of OVII column densities ($N_{OVII} \in [10^{15}, 10^{20}$ cm$^{-2}]$), turbulence velocities ($v_{turb} \in [0,500$ km s$^{-1}]$), and temperatures ($kT \in [1,20$ keV]). The weighted mean

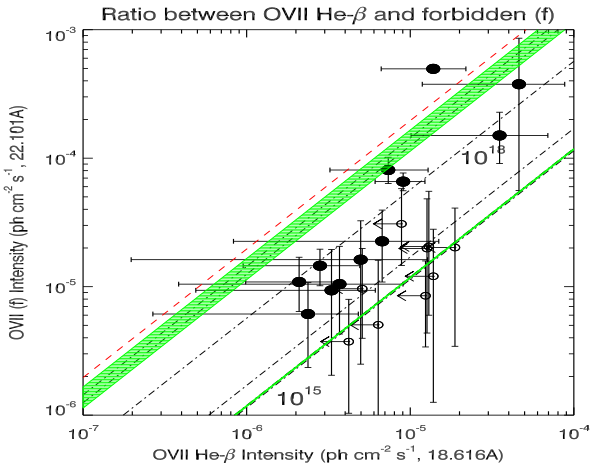

Figure 3. Intensity of OVII He-β transitions against the intensity of the f component of the triplet (only data points corresponding to a detection of the latter are shown; data points correspond to upper limits on the intensity of the former are shown as *empty symbols*). The *dashed-dotted lines* represent the prediction of the `photoion` code for OVII column densities increasing from $N_{OVII} = 10^{15}$ to 10^{20} cm^{-2} in steps of one decade, assuming $kT = 5$ eV and $v_{turb} = 200$ km s^{-1}. The *long-dashed line* (*red*) represents the predictions for pure photoionization. The *shaded areas* (*green*) represent the locii of the `photoion` predictions, when the turbulent velocity varies in the range 0–500 km s^{-1} at constant temperature and for the extreme values of the column density interval. The area representing a variation of the temperature in the range 1–20 keV at constant velocity and column density are comparatively smaller, and therefore not shown.

Table 1
Higher-order intensity ratios for selected transitions in *CIELO*. Each ratio is calculated as the weighted mean of the individual ratios on the N sources, where a measurement of both transitions is available. Expected values for pure photoionization (PIE) and collisional ionization (CIE) are extracted from Tab. 3 in Kinkhabwala et al. (2002)

Ion	Ratio	N	PIE	CIE
CVI Ly-β/Ly-α	0.51 ± 0.32	9	0.14	0.09
OVII He-β/f	0.21 ± 0.13	12	0.05	...
O VIII Ly-β/Ly-α	0.30 ± 0.18	13	0.14	0.10

of the He-β versus f intensity ratio is 0.21 ± 0.13, larger then expected for pure photoionization. It corresponds to OVII column densities $N_{OVII} \simeq 10^{17-18}$ cm^{-2} (the dependence on the other parameters is small). The measurements on the He-β OVII transition at 18.6270Å could be contaminated by the nearby NVII RRC at 18.5872Å. In order to minimize this contamination, we fit the X-ray spectra around the OVII He-β feature in a range, which does not include the contaminating feature. Moreover, we have verified that similar enhancements of higher-order lines to the Lyman-α of H-like Carbon and Oxygen are observed as well (cf. Tab. 1). The dependence on the temperature, column density and velocity distributions in H-like species is such that no meaningful constraints on column density can be drawn. However, in 8 of the individual brightest sources in our sample the ratio between the OVIII Ly-β and Ly-α intensities is large enough to be formally inconsistent with collisional ionization, and in 4 of them with pure photoionization as well.

3.3. AGN and starburst soft X-ray spectra

We have analyzed the RGS spectra of a sample of 27 StarBurst (SB) galaxies extracted from the Wu et al. (2002) sample and observed by XMM-Newton, to identify diagnostic criteria, which may allow us to statistically discriminate between SB- and AGN-dominated soft X-ray spectra. The distribution functions of the luminosity ratio between L shell iron and oxygen He- and H-like integrated lines are indistinguishable (Fig. 4). Kallman et al. (1996) had already pointed out L-shell iron transitions can give an important contribution to the overall luminosity budget in pho-

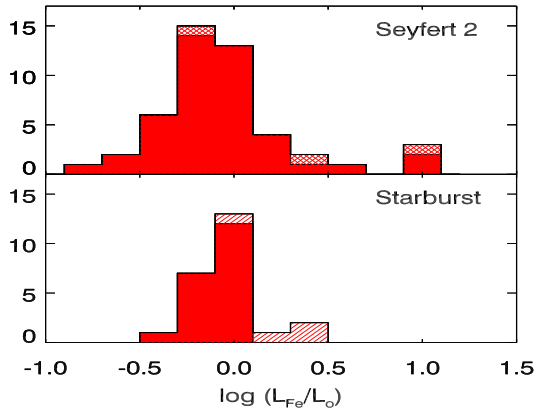

Figure 4. Distribution function for the logarithm of the ratio of the integrated luminosities in the iron and oxygen lines for our Seyfert 2 (*lower panel*) and the control sample of starburst galaxies (*lower panel*). *Diagonally shaded cells* indicate upper limits, *checked cells* indicate lower limits. The median of the two distributions is basically the same: -0.10 and -0.08, respectively.

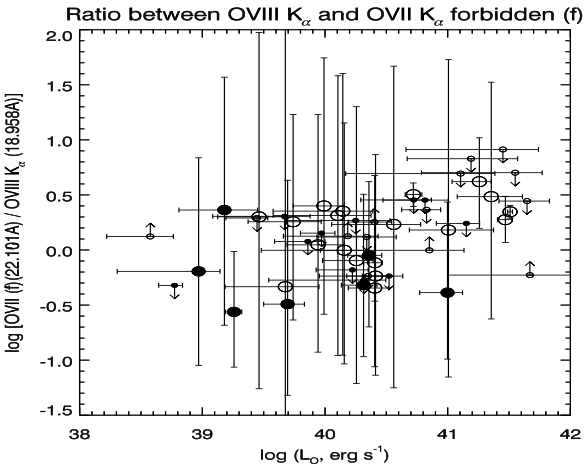

Figure 5. Intensity of the f component of the OVII triplet (normalized to the OVIII Ly-α intensity) against the total luminosity in Oxygen lines. *Empty circles* represents the obscured AGN in *CIELO*, *filled circles* the control sample of 27 starburst galaxies. Symbols representing censored data are plotted with a smaller size for the sake of clarity.

toionized nebulae. Likewise, the standard G ratio ($G \equiv (f+i)/r$; Gabriel & Jordan 1969; Porquet et al. 2000), provide ambiguous diagnostics. Previous studies (cf. Sect. 1) have already shown that the enhancement of resonant lines by resonant scattering mimics the behavior of a weak collisionally ionized plasma, where all the components of the triplet are enhanced with respect to the pure photoionized case, thus decreasing the contrast between the forbidden and the other components, and hence the measured G value. Interestingly enough, the fraction of SB spectra where narrow RRC features are detected is comparable to that observed in the Seyfert 2 sample, indicating that photoionization plays an important role in the ionization balance of starburst galaxies as well.

In Fig. 5 we compare the distribution of the OVII f transition intensity, normalized against the intensity of the OVIII Ly-α, as a function of the total luminosity in oxygen lines (integrated on all He- and H-like transitions), AGN are generally characterized by larger intensity ratios, η: $\eta_{AGN} = 1.38\pm^{0.13}_{0.12}$, $\eta_{SB} = 0.57\pm^{0.07}_{0.09}$ (5.8σ difference; the upper limits have been taken into account with a "bootstrap" method for censored data fit as in Schmitt 1985). The same figure as well shows that the average line luminosity in AGN is larger than in starburst. The median Oxygen lines luminosity is $\sim 10^{41}$ erg s^{-1} in the former and $\sim 10^{40}$ erg s^{-1} in the latter (using strict detections only). Still, the overlap between the line diagnostic distributions is significant, and prevent strong statements on individual sources. This most likely reflects the intrinsic "composite" nature of several obscured AGN [7].

4. Conclusions

1. Radiative Recombination Continua: we detect RRC features in about 40% of the sample source, and in 33% (27%) they allow us to constraint the temperature of the plasma $\leq$ 50 eV ($\leq$ 10) eV. This indicates that in a large fraction of objects in our sample photoionization dominates the ionization balance. Still, these percentages represent probably lower limits to the true fraction of photoionized sources in our sample: upper limits on narrow RRC features in almost 50% of the objects in our sample are still inconclusive due to the lack of statistics

2. Resonant scattering: higher order transitions are enhanced with respect to the expectation of pure photoionization, and as well inconsistent with the expectation of collisional ionization. This indicates that resonant scattering plays an important role in the ionization/excitation balance. The observed OVII He-β versus f intensity ratios are consistent with OVII column densities in the range $N_{OVII} \sim 10^{17-18}$ cm^{-2}. Interestingly enough, these values are in good agreement with the column densities measured in "warm absorbers" observed along the lines of sight to unobscured AGN [4].

3. Starburst contribution: the comparison between the spectra of obscured AGN in our sample and a control sample of nearby starburst galaxies suggests two empirical criteria to discriminate *on a statistical basis* between AGN- from starburst-powered spectra: a) total Oxygen line X-ray luminosities $\gtrsim 10^{40}$ erg s^{-1}; b) ratio between the OVII triplet f component and the OVIII Ly-$\alpha \gtrsim 1$.

The currently available X-ray instrumentation allowed us to explore the nature of the soft X-ray emission in obscured AGN as weak as $\sim$0.01 mCrab. From this study, we have gained confidence that conclusions on the properties of the gas in the circumnuclear region of AGN extracted from the detailed study of high-quality spectra of the brightest objects can be extended to the whole population of nearby obscured AGN. This is the main message we would like to convey with this *paper*, which opens interesting perspectives for future enlargements of this study once deeper exposures or more sensitive instrumentation are available.

REFERENCES

1. Band D.L., Klein R.I., Castor I.J., Nash J.K., 1990, ApJ, 362, 90
2. Bianchi S., Guainazzi M., Chiaberge M., 2006, A&A, 448, 499
3. Bianchi S., Miniutti G., Fabian A.C., Iwasawa K., 2005, MNRAS, 360, 380
4. Blustin A.J., et al., 2003, A&A, 403, 481
5. Brinkman A.C., Kaastra J.C., van der Meer R.J.L., Kinkhabwala A., Behar E., Kahn S., Paerels F.B.S., Sako M., 2002, A&A, 396, 761
6. Cid Fernandes R., Storchi-Bergman T., Schmitt H.R., 1998, ApJ, 501, 94
7. Cid Fernandes R., Heckman T., Schmitt H., Gonzaález-Delgado R.M., Storchi-Bergmann T., 2001, 558, 81
8. der Herder J., et al., 2001, A&A, 365, L7
9. Dickey J.M., Lockman F.J., 1990, ARA&A 28, 215
10. Gabriel A.H., Jordan C., 1969, MNRAS, 145, 241
11. Gabriel C., Denby M., Fyfe D. J., Hoar J., Ibarra A., 2003, in ASP Conf. Ser., Vol. 314 ADASS XIII, eds. F. Ochsenbein, M. Allen, & D. Egret (San Francisco: ASP), 759
12. Gonzalez Delgado R., Heckman T., Leitherer C., 2001, ApJ, 546, 845
13. Guainazzi M., Matt G., Perola G.C., 2005, A&A, 444, 119
14. Kallman T.R., Liedahl D., Osterheld A., Goldstein W., Kahn S., 1996, ApJ, 465, 994
15. King A.R., 2005, ApJ, 635, L121
16. Kinkhabwala A., et al., 2002, ApJ, 575, 732
17. Krolik J.H, Kriss G.A., 1995, ApJ, 447, 512
18. Levenson N.A., Krolik J.H., Życki P.T., Heckman T.M., Weaver K.A., Awaki H., Terashima Y., 2002, ApJ, 573, L81
19. Liedahl D.A, Paerels F, 1996, ApJ, 469, L33
20. Matt G., 1994, MNRAS, 267, L17
21. Porquet D., Dubau J., 2000, A&AS, 143, 495
22. Pounds K.A., Page K.L., 2005, MNRAS, 360, 1123
23. Sambruna R., Netzer H., Kaspi S., Brandt W.N., Chartas G., Garmire G.P., Nousek J.A., Weaver K.A., 2001, ApJ, 546, L13
24. Sako M., Kahn S.M., Paerels F., Liedahl D.A., 2000, ApJL 543, L115
25. Schmitt J.H.M.M., 1985, A&A, 293, 178
26. Schurch N.J., Warwick R.S., Griffiths R.E, Kahn S.M., 2004, MNRAS, 350, 1
27. Turner T.J., George I.M., Nandra K., Mushotzky R.F., 1997, ApJS 113, 23
28. Young A.J., Wilson A.S., Shopbell P.L., 2001, ApJ, 556, 6
29. Wu W., Clayton G.C., Gordon K.D., Misselt K.A., Smith T.L., Calzetti D., 2002, ApJS, 143, 377

ACKNOWLEDGMENTS

The authors are deeply grateful to Dr.H.Kinkhabwala, for providing us with an updated version of his `photoion` code, as well as for several enlightening and encouraging suggestions and comments.